

# The Edar subfamily in feather placode formation



Available online at www.sciencedirect.com
ScienceDirect
Developmental Biology 305 (2007) 232–245
DEVELOPMENTAL BIOLOGY
www.elsevier.com/locate/ydbio

# The Edar subfamily in feather placode formation

Caroline F. Drew [a], Chih Min Lin [b], Ting Xin Jiang [b], Geoff Blunt [a], Chunyan Mou [a], Cheng Ming Chuong [b], Denis J. Headon [a,*]

[a] Faculty of Life Sciences, University of Manchester, Oxford Road, Manchester, M13 9PT, UK
[b] Department of Pathology, Keck School of Medicine, University of Southern California, Los Angeles, CA 90033, USA

Received for publication 24 October 2006; revised 17 January 2007; accepted 9 February 2007
Available online 16 February 2007

**Abstract**

A subgroup of the TNF receptor family, composed of Edar, Troy and Xedar, are implicated in the development of ectodermal appendages, such as hair follicles, teeth and sweat glands. We have isolated chicken orthologues of these three receptors and analysed their roles in early feather development. Conservation of protein sequences between mammalian and avian proteins is variable, with avian Edar showing the greatest degree of sequence identity. cXedar differs from its mammalian orthologue in that it contains an intracellular death domain. All three receptors are expressed during early feather morphogenesis and dominant negative forms of each receptor impair the epithelial contribution to feather bud morphogenesis, while the dermal contribution appears unaffected. Hyperactivation of each receptor leads to more widespread assumption of placode fate, though in different regions of the skin. Receptor signaling converges on NF-κB, and inhibiting this transcription factor alters feather bud number and size in a stage-specific manner. Our findings illustrate the roles of these three receptors during avian skin morphogenesis and also suggest that activators of feather placode fate undergo mutual regulation to reach a decision on skin appendage location and size.


*Keywords:* TNFR; Placode; Feather; Skin; Evolution; Death domain; Edar; Troy; Xedar

## Introduction

Skin appendages, such as hairs, feathers, scales and glands, are class-defining features in vertebrates. While the skin itself forms a barrier, its appendages play a wide variety of roles, from defence and display to insulation and aerodynamics. During development these cutaneous appendages are laid out in a periodic pattern in the embryonic ectoderm, the cells of which must all choose between appendage and surface keratinocyte fates. The cells that will become appendages first condense to form dense patches, called placodes. After placode specification, cell proliferation generates downgrowths in mammals to produce hair follicles (Hardy, 1992), or outgrowths in birds to produce a feather bud (Lin et al., 2006). The process of appendage formation in all vertebrate classes relies on a series of reciprocal interactions between the epidermis and its underlying dermis (Sengel, 1990; Hardy, 1992; Fuchs et al., 2001; Millar, 2002).

In mouse, hair follicles are generated across the entire surface of the embryo in a series of temporally defined pulses late in gestation, the later forming follicles filling in the gaps that open up between older follicles as the skin grows. In contrast, in avian skin, several tracts are formed first; following which a defined morphogenetic wave moves across specific tracts, leaving a very regular array of placodes in its wake (Jiang et al., 2004). Despite the similarities between early hair and feather follicle morphogenesis, they appear to be convergently evolved structures (Wu et al., 2004).

The formation of feather buds takes place in hierarchical levels (Chang et al., 2004). In the first level, feather fields (which later become feather tracts) form from presumptive dermis and ectoderm. In the second level, periodic patterning takes place and the originally homogeneous feather field breaks into individual feather buds and interbud regions. In the subsequent levels, feather buds undergo morphogenetic events

* Corresponding author.
*E-mail address:* denis.headon@manchester.ac.uk (D.J. Headon).

0012-1606/$ - see front matter © 2007 Elsevier Inc. All rights reserved.
doi:10.1016/j.ydbio.2007.02.011

to form an anterior–posterior axis and branches (Yu et al., 2004; Lin et al., 2006).

The expression pattern of genes involved in periodic pattern formation can be categorized into two distinct modes, 'restrictive' and 'de novo', reflecting the successive stages of their functions (Jiang et al., 2004). Molecules with 'restrictive' expression are involved in negotiating placode position. They are initially expressed homogeneously at a moderate level. As appendage locations are specified, these genes become restricted to or upregulated in the placodes and downregulated in the surrounding regions, or vice versa. *β-Catenin* is an example and is considered to be required for establishing the competence of feather field. Molecules with 'de novo' expression, such as *Shh*, appear directly in the placode once its position has been defined. They serve to regulate bud growth, shaping, axis determination and outgrowth morphogenesis (Jiang et al., 1999; Widelitz et al., 2000). The molecules involved in pattern formation fall into two functional categories, i.e. activators and inhibitors of placode fate. Whether direct or indirect, interactions between these inhibitors and activators are responsible for breaking the symmetry of the early skin into the hexagonal feather pattern that emerges (Jiang et al., 2004).

The tumour necrosis factor receptor (TNFR) family is expanded in the vertebrate lineage, with mammalian genomes containing about 30 members (Locksley et al., 2001), compared to a single gene in *Drosophila* (Kanda et al., 2002). This expansion appears to be correlated with acquisition of roles in vertebrate evolutionary novelties, such as the adaptive immune system, bone, mammary gland, and skin appendages (Locksley et al., 2001). The TNFR family can be subdivided in two ways. Several subfamilies are defined by sequence similarities in the receptors' extracellular ligand binding domains, with each subfamily being a product of gene duplication and divergence (Locksley et al., 2001). Alternatively, TNFR family members can be allocated to one of two functional classes according to their mode of signaling, which depends on whether they contain an intracellular death domain or not. Eight receptors (Edar, p75 NGFR, TNFR1, Fas, DR3, DR4, DR5, and DR6), which are scattered among the subfamilies, contain a C-terminal death domain which is used to recruit cytoplasmic death domain adaptor proteins (Wajant, 2003). These adaptors in turn recruit members of the Traf family to transduce signals, commonly resulting in activation of the transcription factor NF-κB, and sometimes initiating apoptosis. A majority of TNFRs do not contain a death domain and initiate signaling by recruiting Trafs directly to their cytoplasmic tails (Inoue et al., 2000).

Ectodysplasin (Eda) is a member of the TNF family of ligands and it was initially implicated in appendage development by the cloning of a gene underlying hypohidrotic ectodermal dysplasia (HED) in mouse and human (Kere et al., 1996; Thesleff and Mikkola, 2002). HED is characterized by agenesis or malformation of ectoderm-derived appendages, such as teeth, sweat glands and hair follicles, while the skin itself develops normally. Positional cloning identified a receptor for Eda, a member of the TNFR superfamily called Edar (Headon and Overbeek, 1999), and a cytoplasmic transducer of Edar signals called Edaradd (Headon et al., 2001; Yan et al., 2002). Like the ligand, Eda, both receptor and adaptor are mutated in mouse and human HED. Mice with genetic lesions that affect this signaling pathway display a phenotype in which primary hair follicles, normally developing between embryonic day 14 (E14) and E16, are entirely absent, while the later developing secondary hair follicles are almost normal (Headon and Overbeek, 1999; Laurikkala et al., 2002). Therefore, the Eda pathway is required specifically for initiation of primary hair follicles, while whiskers and secondary follicles are minimally affected by its absence. A reciprocal phenotype is caused by mutation of the transcription factor Lef-1 or the BMP inhibitor Noggin, which are required to initiate development of secondary, but not primary, hair follicles (van Genderen et al., 1994; Botchkarev et al., 2002; Plikus et al., 2004). Thus two genetically distinct pathways are utilized to activate hair follicle development at different stages of mouse development. Interestingly, Lef-1, Noggin and the Eda pathway components are all expressed in both primary and secondary follicle placodes, and so their expression characteristics do not indicate their functional roles in a given follicle subtype. Though the evolutionary relationships between ectodermal appendages in different vertebrate classes are unclear, a conserved role for Edar signaling in their development is indicated by the finding that its mutation underlies a spontaneous fish mutant that lacks scales (Kondo et al., 2001).

Following identification of Edar, two novel TNFRs, Troy and Xedar, were cloned and found to be expressed in the embryonic epidermis and appendages (Kojima et al., 2000; Yan et al., 2000). The extracellular domains of Edar, Troy and Xedar mark them out as a distinct subfamily within the TNFRs, though their intracellular domains are unrelated to one another (Locksley et al., 2001). Xedar binds to a specific splice variant of Eda, EdaA2, which differs by two amino acids from the Edar binding variant, EdaA1 (Yan et al., 2000). No TNF ligand has been identified for Troy (Bossen et al., 2006). All three receptors employ Trafs, which ultimately leads to activation of NF-κB (Kojima et al., 2000; Yan et al., 2000). However, while Edar contains a death domain used to recruit Edaradd for signal transduction, this domain is entirely absent from the mammalian Troy and Xedar proteins. Recent studies of null mutations in Xedar and Troy have reported an absence of gross skin or appendage phenotypes (Newton et al., 2004; Shao et al., 2005).

Previous work has described the expression of *cEda*, *cEdar* and *cEdaradd* in the forming feather field and showed that ectopic activation of cβ-catenin was sufficient to induce *cEdar* expression (Houghton et al., 2005). Here we describe the effects of suppression and activation of Edar and its related receptors in developing chicken skin *in vitro* and *in vivo*, and the effects of suppression of NF-κB activity. This work defines functional roles for signaling from these receptors, and for NF-κB, in feather development. Our findings also suggest a mutual feedback regulation among activators in the periodic patterning process. It is perhaps the summation of these activities that specify the placode and inter-placode fates, rather than the linear cβ-catenin–cEdar axis proposed in previous studies (Houghton et al., 2005).

## Materials and methods

### *Isolation of chicken cDNAs*

Chicken EST databases (Boardman et al., 2002) were queried using human Eda, Edar, Edaradd, Troy and Xedar amino acid sequences. Available sequences were used to design oligonucleotides for 5′ and 3′ RACE to generate cDNAs covering a full-length ORF. RACE ready cDNA was generated from E8 chicken skin using the Generacer kit (Invitrogen). When the first round of RACE did not give discrete products a nested reaction was performed. Oligonucleotides used were:

cEda5′S: 5′-CCTTTCTGCAATGCACTCGGAGTA-3′; cEda5′SN: 5′-CCACGCTGACATCTCCATCAACATGA-3′; cEda3′AS: 5′-TCATCTAG-GATGCTGGCGCATCTC-3′; cEda3′ASN: 5′-GATGGAGATGT-CAGCGTGGACCAT-3′
cTroy 5′S: GGGCCTGTTCATTTGATTCCTTCACT-3′
cXedar5′S: 5′-GTGCACCGAGCTCGACCTGCAGAA-3′; cXedar5′SN: 5′-AGATGGAGTTTGTGAGCAGTGAGC-3′; cXedar3′AS: 5′-GCTCACTGCTCACAAACTCCATCT-3′

Sequences for *cEdar* were not represented in the EST database therefore a partial sequence within the death domain between amino acids 372 and 387 was obtained by degenerate PCR. This sequence was then extended by 5′ and 3′ nested RACE reactions.

cEdar5′S: 5′-GTGGTGAAAACGTGGCGTCACCTT-3′;
cEdar5′SN: 5′-CTTTGGGCTGAAGAGGGACGAGAT-3′;
cEdar3′AS: 5′-ATCTCGTCCCTCTTCAGCCCAAAG-3′;
cEdar3′ASN: 5′-CTCTCCGCAAGGTGACGCCACGTT-3′.

Novel sequences have been submitted to GenBank (cTroy-long DQ360499, cTroy-short DQ360500, cXedar DQ360501).

### *RT–PCR*

Epidermis was separated from dermis using dispase and RNA isolated from each tissue using TRI reagent (Sigma). cDNA was synthesized using random primers (Invitrogen) and AMV reverse transcriptase (Roche). The *cEda* RT–PCR was run on a 4% agarose gel to distinguish the A1 and A2 forms, which differ in size by 6 nucleotides. For quantitative RT–PCR cDNA was generated from 3 individual embryos for each age examined. Quantification of *18S* rRNA was used to normalize *Eda* expression levels. For each cDNA sample three 20 μl reactions containing SYBR green (Molecular Probes) were run on an Opticon 2 thermal cycler (MJ Research) under the following conditions: 95 °C for 19 min (×1), 95 °C for 15 s; 59 °C for 39 s; 72 °C for 39 s (×40). The following primers were used for amplification:

cEdar ATG S: 5′-CCATCGATTATCAAGAGAACATGGCTCAC-3′
cEdar 322AS:5′-CCATCGATTCAAATCCCAGTTGATTTATTGC-3′
cTroy ATG S: 5′-CCATCGATAAGAAATGGATCCTAAAGG-3′
cTroy PstI200AS: 5′-ATACTGCAGTTTCTTCTCCATAAACTGCC-3′
cXEdar RT S: 5′-AGGACTGTGGTGATGGTGTG-3′
cXEdar RT AS: 5′-TGAACTGAACTGCTTCCACT-3′
cβ-Catenin S: 5′-ACCCAAGCTGACTTGATGGAGTTG-3′
cβ-Catenin AS: 5′-CAGCCAGGCGCTGCACATTAGTTG-3′
cFGF10 S: 5′-TCTTCTGTGCCTGTCACCTG-3′
cFGF10 AS: 5′-TTGCCTTCCATTGTGCTTCC-3′
cEda A1/A2 S: 5′-TGGTCTCGCATCACTATGAAC-3′
cEda A1/A2 AS: 5′-AATACTCCGAGTGCATTGCAG-3′
18S rRNA S: 5′-TCAGATACCGTCGTAGTTCC-3′
18S rRNA AS: 5′-TTCCGTCAATTCCTTTAAGTT-3′

### *Whole mount in situ hybridization*

Whole mount in situ hybridizations were carried out on White Leghorn or scaleless mutant (University of Connecticut, Storrs, CT) embryos using digoxigenin-labelled riboprobes as described (Riddle et al., 1993), with a proteinase K treatment of 5 μg/ml for 5 min. The templates used to generate riboprobes were: *cβ-catenin*: codons 1–127; *cEda*: 80 nt of ORF and 333 nt of 3′UTR; *cEdar*: entire ORF and 43 nt of 5′ and 3′UTRs; *cTroy*: codons 17–257; *cXedar*: 202 nt of 5′UTR and codons 1–337. To identify feather placodes, embryos were stained with 0.02% ethidium bromide as described (Eames and Schneider, 2005). For detection of viral proteins after in situ hybridization, stained embryos were processed for cryosectioning by snap-freezing tissue in OCT (Sakura Tissue-Tek) in liquid nitrogen. Immunostaining was performed on 16 μm cryosections using the anti-gag antibody AMV3C2 (D. Boettiger, Developmental Studies Hybridoma Bank, University of Iowa) at a 1:750 dilution followed by antibody detection using the Vectastain ABC kit (Vector) and Sigma*FAST* 3,3′-diaminobenzidine.

### *Western blotting*

E14 wild type, $Eda^{Ta/Ta}$ and $Edaradd^{cr/cr}$ mouse, and E8 chicken dorsal, skins were dissected, homogenized in TRI reagent and proteins isolated. Samples were run on an 18% SDS–PAGE gel and transferred to a nitrocellulose membrane. Rabbit anti-Eda antibody (AL166, produced by immunization using mouse Eda amino acids 245–391, Schneider et al., 2001) was used at 1/1000, anti-mouse HRP secondary at 1/10,000 (Amersham) and mouse monoclonal anti-β*Actin*–horseradish peroxidase at 1/25,000 (AC-15, Sigma). Signal was detected using SuperSignal West Pico Chemiluminescent Substrate (Pierce).

### *Generation of proviral constructs*

Dominant negative receptors were generated by replacing intracellular signaling domains with enhanced green fluorescent protein (GFP, amplified from pEGFP, Clontech). DN-cEdar consisted of amino acids 1–292, DN-cTroy amino acids 1–200, and DN-cXedar amino acids 1–167.

Constitutively active receptors were generated by fusing a cDNA encoding the six transmembrane domains of the Epstein–Barr viral LMP1 protein (codons 1–188) to the receptors' intracellular domains (*cEdar* codons 213–448, *cTroy* codons 193–409, *cXedar* codons 161–504). The *LMP1* cDNA was amplified from a pSG5:LMP1 template (from Bill Sugden, University of Wisconsin).

Fused cDNA PCR products were cloned into the pCR8/GW/TOPO Gateway entry vector (Invitrogen) and sequenced. An LR recombination reaction was performed to transfer the cDNAs to a Gateway compatible RCASBP (A) vector (Loftus et al., 2001).

### *Preparation of RCAS virus*

DF-1 cells (from C. Tickle, University of Dundee) were cultured in DMEM/10% FBS and transfected with proviral plasmid DNA using Lipofectamine 2000 (Invitrogen). When infected cells reached confluence the medium was replaced with a minimal volume of DMEM/1% FBS, which was collected after 24 h and filtered through a 0.45-μm filter. The filtrate was used directly for *in ovo* injections.

### *NF-κB reporter assay*

RCAS-infected DF-1 cells were cultured for 7 days and then cotransfected with a 10:1 molar ratio of the pNF-κBluc reporter plasmid (Clontech) and the pRL-TK (*Renilla* luciferase) plasmid (Promega). Luciferase activity was measured 18 h after transfection using the Dual Luciferase Reporter Assay System (Promega).

### *Viral transduction of reconstituted skin explants*

Reconstitution assays were performed as described (Jiang et al., 1999). Dorsal skins from stage 31 white leghorn embryos were dissected in HBSS and incubated in 2× calcium/magnesium free medium with 0.25% EDTA. Epithelium and mesenchyme were separated and the mesenchyme was incubated in 0.1% collagenase/trypsin for 10 min at 37 °C to prepare a single-cell suspension. Cells were pelleted by centrifugation and resuspended in virus containing medium for 1 h. Reconstituted explants were made by plating mesenchymal cells at high density on tissue culture inserts and then placing the

intact epithelium back on top of the mesenchyme. The reconstituted explants were cultured in DMEM/10% FCS and incubated at 37 °C in 5% $CO_2$.

### *In ovo injection*

Conditioned media from RCAS-infected cultures were used to inject stage 20 embryos *in ovo*. Approximately 5 μl of viral suspension was delivered between the amniotic membrane and the dorsal ectoderm of the embryos between the wing and limb buds. Embryos were harvested at E8, fixed in 4% PFA in PBS overnight at 4 °C, then processed for *in situ* hybridization. Numbers of embryos analysed were: CA-cEdar ($n$=35), CA-cTroy ($n$=31), CA-cXedar ($n$=14), DN-cEdar ($n$=16; 7 with bud suppression phenotype=44%), DN-cTroy ($n$=15; 6 with bud suppression phenotype=40%), DN-cXedar ($n$=19; 5 with bud suppression phenotype=26%), GFP control ($n$=12) and LMP1 control ($n$=12). The presence of virus was monitored by detection of GFP-positive foci or by antibody staining to detect the viral gag protein.

### *NF-κB inhibition*

Dorsal skin was dissected from E7 embryos, placed on a culture insert and treated with 1 μl/ml DMSO (control) or 100 μM NF-κB inhibitor BAY 11-7082 (Sigma Aldrich) dissolved in DMSO. Explants were photographed and processed for sectioning and in situ hybridization.

## Results

### *Cloning and expression of the chicken Edar subfamily*

We used the sequences of human Eda, Edar, Troy and Xedar to query chicken EST sequence databases and verified full-length ORFs by 5′ and 3′ RACE. This approach identified a single orthologue for each component of the mammalian Edar signaling pathway and its related receptors (Fig. 1A). The predicted extracellular domains of Edar, Troy and Xedar were all well conserved between chicken and human (Edar 84%, Troy 79%, Xedar 65%), while the degree of conservation of their intracellular domains was much more variable (Edar 85%, Troy 48%, Xedar 14%). We identified two forms of cTroy which differ in the length of their intracellular domains (217 versus 66 cytoplasmic amino acids), comparable to the long and short Troy isoforms described in mammalian genomes (223 versus 21 cytoplasmic amino acids) (Kojima et al., 2000). Troy-short may represent an endogenous dominant negative form or a receptor with a distinct signaling output.

As in mammals, the extracellular domains of cTroy and cXedar are more closely related to one another than either is to cEdar. Also, cEdar and cTroy, and cTroy and cXedar, have no detectable sequence similarity in their intracellular domains. In contrast to the mammalian proteins, however, cXedar contains within its last exon a region that is similar to the death domain of cEdar. Conservation of key amino acid residues between this region of cXedar and the death domains of human EDAR and p75 NGFR, as well as its location in the protein, confirm that this is a death domain (Fig. 1B). Thus between avian and mammalian lineages the Edar sequence and domain structure is highly conserved, the Troy protein moderately so, and Xedar is highly diverged.

We examined the expression pattern of each of these genes during early feather development. RT–PCR at incubation day 8 (E8) detected *cEdar* and *cTroy* specifically in the epidermis, while *cXedar* was present in both epidermis and dermis (Fig. 1C). Whole mount in situ hybridization revealed that *cEdar* and *cTroy* have similar expression characteristics. Both genes are expressed in the primary row of the spinal tract at E6 (Figs. 1D, E) and, at E7, they are expressed in the placodes and the morphogenetic wave (Figs. 1F, G). Thus *cEdar* and *cTroy* both undergo the restrictive mode of expression, from homogenous staining in the morphogenetic wave to upregulation in the placodes. In the humeral tracts at E7 the two receptors are expressed in placodes (Figs. 1H, I), but *cEda* mRNA is detected in the interplacode region (Fig. 1J), as previously reported (Houghton et al., 2005). In the scaleless mutant fowl, which almost completely lacks the morphological and molecular indications of feather development, *cEdar*, *cTroy* and *cEda* are all expressed diffusely (Figs. 1K–M), as previously described for other genes expressed in the restrictive mode (Widelitz et al., 2000). In E8 humeral tracts *cEdar* and *cTroy*, but not *cXedar*, were expressed in a punctate expression pattern (Figs. 1N–P), but by E10 all three receptors are upregulated in the outgrowing short buds (Figs. 1Q–S). *cEdar* and *cTroy* are also expressed in foot scales (Figs. 1T, U), with *cEda* transcript in a reciprocal pattern in the interscale region (Fig. 1V).

The sequence conservation and expression characteristics of *Edar*, *Troy* and *Xedar* between mammals and birds suggest that they may play similar, yet distinct, roles in skin development across amniote lineages.

### *Eda splice variants and protein solubilization*

Eda is produced in two functionally distinct splice forms; the EdaA1 protein specifically activates Edar, while EdaA2, which lacks 2 amino acids present in the A1 form, activates Xedar (Yan et al., 2000). We performed RT–PCR using oligos adjacent to this alternative splice site to estimate the relative abundance of each isoform during development. Both isoforms are expressed in epidermis and dermis, with the *EdaA1*:*EdaA2* ratio essentially constant through development (Fig. 2A). Thus in this system alternative splicing of *Eda* appears to be a constitutive event, with no evidence of temporal or spatial regulation. Quantitative RT–PCR detected higher levels of total *Eda* transcript in the dermis than in the epidermis at E7 and E10 (Fig 2B). Eda is synthesized as a transmembrane protein, but cell culture studies have demonstrated that it can be released into the medium by furin-mediated cleavage at an extracellular site (Schneider et al., 2001). To determine whether this cleavage occurs *in vivo*, we first validated an anti-Eda polyclonal antibody by detecting Eda protein in extracts of wild type and $Edaradd^{cr/cr}$ embryonic mouse skin. $Eda^{Ta/Ta}$ samples were used as a negative control to confirm the specificity of the antibody (Fig. 2C) as the genetic lesion in this line removes the *Eda* promoter and first exon (Srivastava et al., 1997). Immunodetection of proteins from developing chicken and mouse skin indicated that Eda is present in both species in the cleaved soluble form (Fig. 2D). As the *cEda* transcript is detected in the interbud domain, with *cEdar* expressed in the placodes (Figs. 1H, J), this solubilization of cEda would allow stimulation of cEdar signaling within the placode.

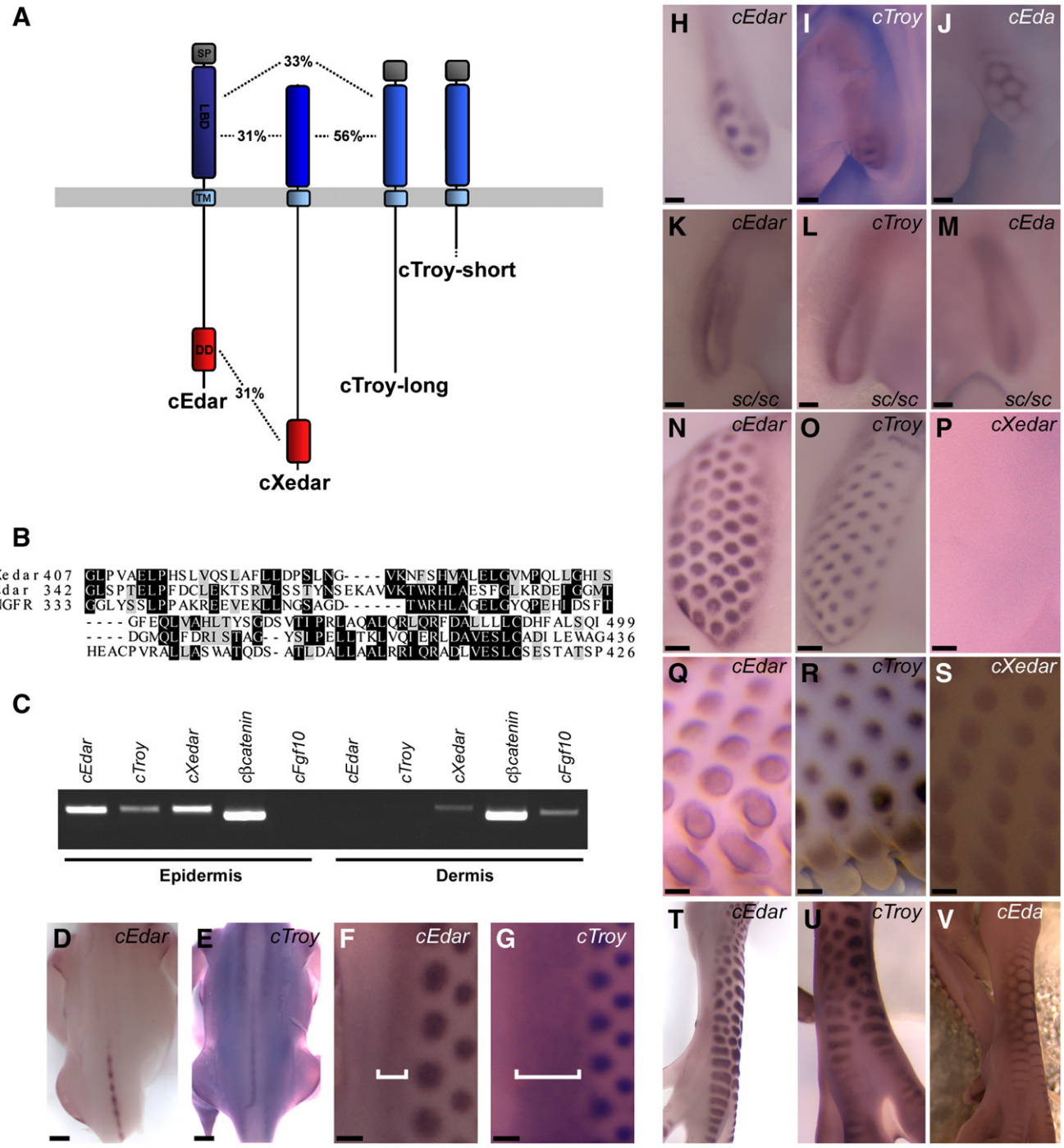


Fig. 1. The chicken Edar subfamily and its expression during skin development. (A) Schematic of cEdar, cXedar, cTroy-long and cTroy-short proteins. Sequence similarities (% amino acid identity) between domains are indicated. The 13 C-terminal amino acids of cTroy-short (dotted line) do not align with cTroy-long. DD, death domain; LBD, predicted ligand binding domain; SP, signal peptide; TM transmembrane domain. (B) Alignment of chicken Xedar with human EDAR and p75 NGFR death domains. Amino acid numbers are indicated. (C) RT–PCR detection of indicated genes in E8 epidermis and dermis. *cEdar* and *cTroy* are specifically expressed in epidermis, while *cXedar* is expressed in both tissues. *cFgf10* is a dermis-specific control. (D) *cEdar* and (E) *cTroy* transcripts are detected along the primary row of the spinal tract at E6 by in situ hybridisation. (F) *cEdar* and (G) *cTroy* are focally upregulated in the placodes of the spinal tract and diffusely expressed in the morphogenetic wave (bracketed) at E7. (H) *cEdar* and (I) *cTroy* are focally expressed in E7 humeral tracts, while (J) *cEda* expression is limited to the interplacode zone. (K–M) None of these genes are focally expressed in humeral tracts of *scaleless* (*sc*/*sc*) mutant skin at E7. At E8 in the humeral tract (N) *cEdar* and (O) *cTroy* remain expressed in placodes, while (P) c*Xedar* is not focally detected. (Q) *cEdar*, (R) *cTroy* and (S) *cXedar* are expressed at E10 as placodes grow out into buds. (T) *cEdar* and (U) *cTroy* are expressed in developing scales at E10, while (V) *cEda* is expressed in the interscale region. Scale bars: D, E = 500 μm; F–S = 150 μm.

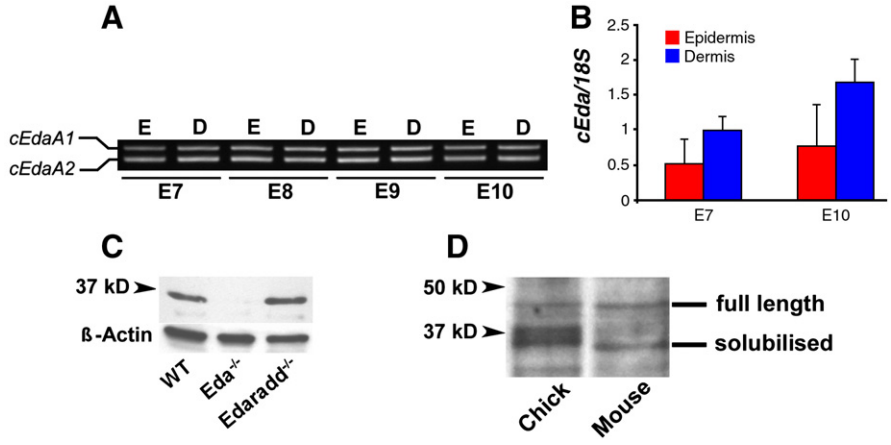


Fig. 2. Analysis of the *Eda* isoforms in feather tract development and detection of solubilised Eda protein *in vivo*. (A) Detection of *cEdaA1* and *cEdaA2* in embryonic epidermis and dermis by RT–PCR. The ratio of A1:A2 shows little variation through feather development at ages E7–E10. E, epidermis; D, dermis. (B) Quantitative RT–PCR determination of *Eda* levels in epidermis and dermis at E7 and E10. Error bars indicate S.E.M. (C) Detection of solubilised Eda in embryonic mouse skin from E14 wild type, $Eda^{Ta/Ta}$ mutant and $Edaradd^{cr/cr}$ mutant mice. (D) Western blot detection of full-length and soluble Eda in E8 chick and E14 wild type mouse skin.

*Reagents to manipulate receptor signaling*

To examine the functions of cEdar, cTroy and cXedar in feather bud development we engineered dominant negative (DN) and constitutively active (CA) forms of each protein (Fig. 3A). To suppress receptor signaling we replaced intracellular signaling domains with GFP. These truncated proteins should sequester wild type receptors into non-functional complexes, analogous to the mode of action of the spontaneous $Edar^{Sleek}$ dominant allele in mouse (Headon and Overbeek, 1999). GFP tagging allows visualization of sites of viral infection and transgene expression.

Activation of receptor signaling could be achieved by overexpressing the native receptors, though with this approach signaling may be influenced by ligand availability. Therefore, we engineered chimeric proteins consisting of the six transmembrane domains of latent membrane protein 1 (LMP1) fused to the receptors' intracellular domains (Fig. 3A). LMP1 is an Epstein–Barr virus encoded protein that self-aggregates in the cell membrane and mimics a constitutively active TNFR (Hatzivassiliou et al., 1998). Thus the chimeric receptors are predicted to display ligand independent signaling.

We tested the NF-κB activation capabilities of the fusion proteins by an NF-κB reporter assay in chicken DF-1 cells. Fusion of receptor intracellular domains to LMP1 activated NF-κB in the case of cEdar and cTroy, while the cXedar fusion protein induced only weak, though statistically significant, activation. Dominant negative receptors displayed no NF-κB activation above the basal level for GFP virus-infected cells, confirming ablation of key signaling domains (Fig. 3B).

*Modulating receptor signaling in reconstituted skin*

We first tested the effects of the cEdar and cTroy on feather bud formation in an *ex vivo* assay. Dissociation of embryonic skin removes placode positional information and allows manipulation of periodic patterning from its initial stages. Also, it allows efficient viral infection in culture. Upon reaggregation, the skin goes on to produce an array of outgrowing feather buds (Jiang et al., 1999). Transduction of

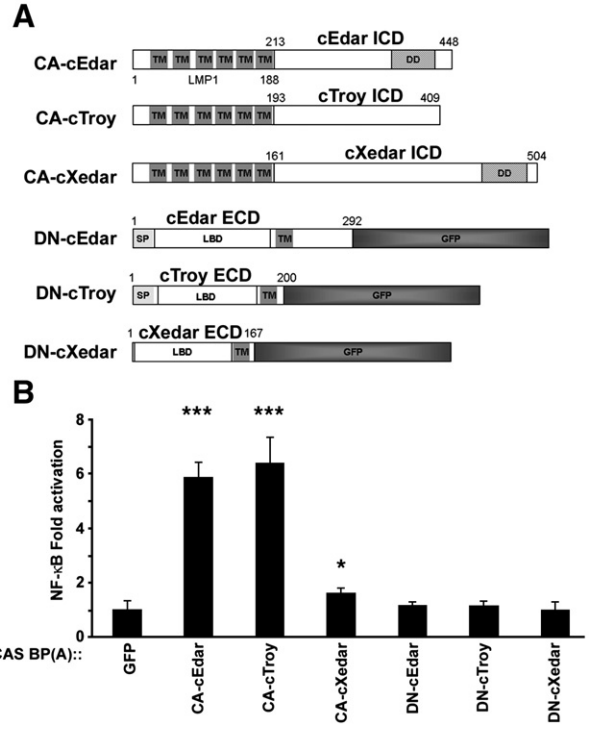


Fig. 3. Design and evaluation of reagents to manipulate receptor signaling. (A) Constitutively active (CA) cEdar, cTroy and cXedar were generated by fusing their intracellular domains (ICD) to the transmembrane domains of LMP1. Dominant negative (DN) receptors were generated by fusing their extracellular (ECD) and transmembrane domains to GFP. DD, death domain; GFP, green fluorescent protein; LBD, predicted ligand binding domain; SP, signal peptide; TM, transmembrane domain. (B) Evaluation of modified receptor signaling. NF-κB-luciferase reporter activation in chicken DF-1 cells infected with indicated RCAS constructs. Expression of CA-cEdar, CA-cTroy and CA-cXedar stimulate NF-κB activity. DN receptors yield no activation above basal levels. Error bars indicate S.E.M. *$p<0.05$, ***$p<0.001$.

reconstituted cultures with RCAS carrying DN-cEdar ($n=12$) or DN-cTroy ($n=8$) inhibited feather bud outgrowth when compared to the effects of control virus at day 2 (Figs. 4A–E). In the transduced explants placode formation was initiated and dermal condensations were visible (Fig. 4E, arrowheads), however, bud outgrowth and development to the short bud stage was not sustained. After 5 days in culture there were no short buds formed while in control explants short buds had elongated to the long bud stage (data not shown). These data suggest therefore that the earliest placode specification stage appears to occur with suppressed cEdar or cTroy signaling, however, placodes fail to progress beyond this stage and after 5 days in culture retain only dermal placode components (Fig. 4E).

Introduction of CA-cEdar during this patterning process yielded a more tightly packed feather array ($n=12$, Figs. 4F–H). CA-cEdar-expressing cultures contained both small (Fig. 4G, arrowheads) and large buds. The larger buds appeared after 24 h in culture, similar to the control. The smaller buds emerged after an additional 24 h, representing a second wave of bud formation

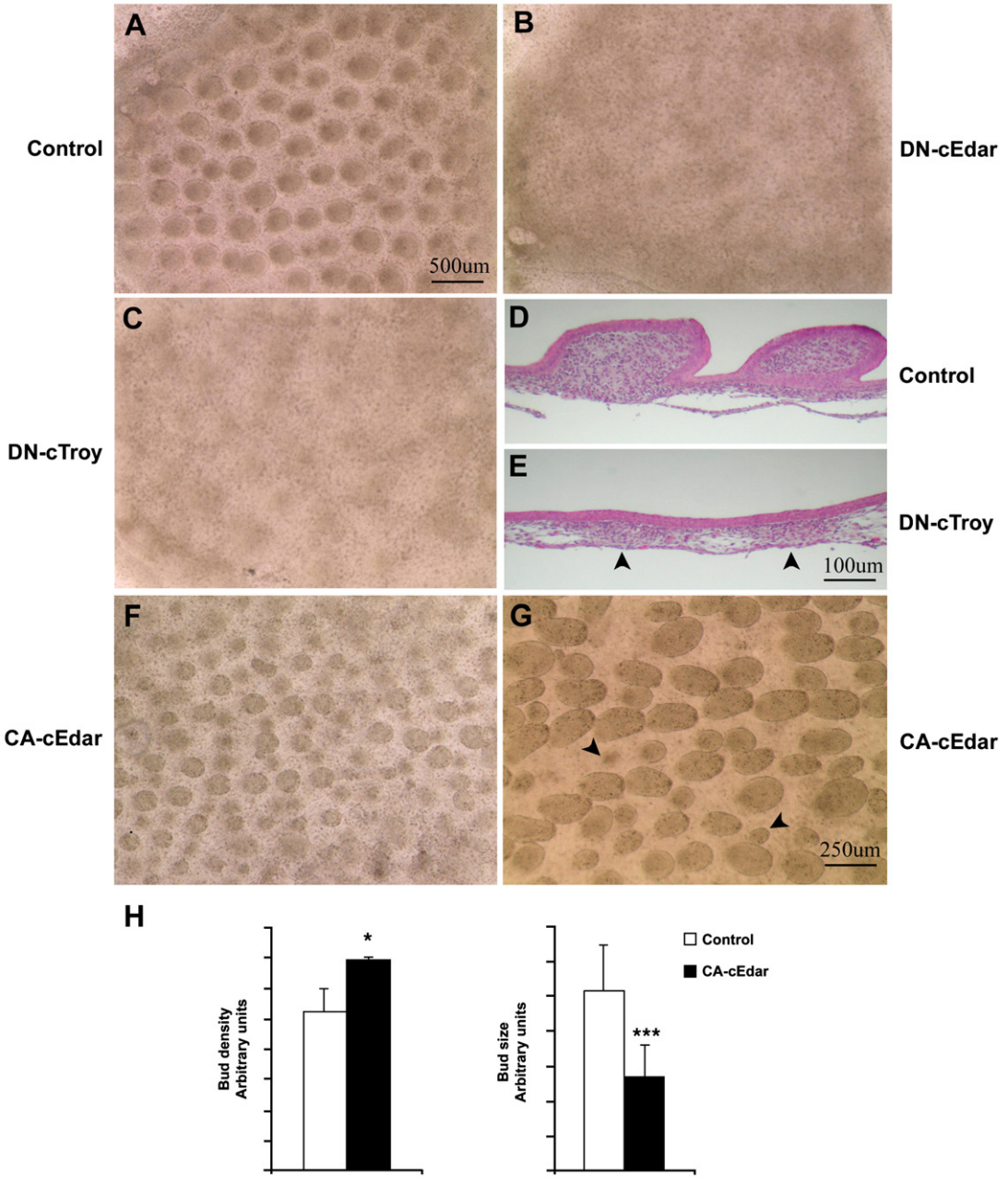


Fig. 4. Manipulation of signaling in skin reconstitution assays. Feather buds after two days in culture. (A) Reconstituted skin transduced with control RCAS virus. Explants transduced with (B) DN-cEdar or (C) DN-cTroy exhibit an overall suppression of bud outgrowth, though feather rudiments can be seen. Sections through (D) control compared to (E) DN-cTroy-infected explants reveal that the formation of epithelial placodes and bud outgrowth is inhibited by suppression of receptor signaling, though dermal condensations have formed (arrowheads). (F) CA-cEdar transduced explant and (G) higher magnification image, showing greater density of buds compared to the control, with a second wave of buds appearing in the interbud region 24 h later (arrowheads). (H) Quantification of feather bud density and size in control and CA-cEdar-infected explants. Error bars indicate standard deviation. *$p<0.05$, ***$p<0.001$. Scale bars: A–C, F=500 μm; D, E=100 μm; G=250 μm.

(Figs. 4F, G). Quantification showed that the bud density increases, but the average size decreases (Fig. 4H). Thus in this *in vitro* model, inhibition of receptor signaling suppresses bud morphogenesis, but does not abolish the initial dermal condensation, while increased receptor activity leads to an increase in bud density.

*In vivo suppression of cEdar subfamily signaling*

We infected embryos *in ovo* with RCAS expressing dominant negative receptors. Phenotypes of embryos with GFP positive patches were assessed by detection of *cβ-catenin* at incubation day 8. *cβ-Catenin* undergoes the restrictive mode of expression and so can be used to visualize both placode fate and the location of the morphogenetic wave (Widelitz et al., 2000). Expression of GFP alone in control embryos did not perturb placode development, while DN-cEdar, DN-cTroy and DN-cXedar all suppressed placode identity, resulting in weak or occasionally absent *cβ-catenin* expressing foci in tracts (Figs. 5B, D, G). The buds with weakened expression that were detectable retained their spatial fidelity. The phenotypes correlated with GFP positive regions and thus transgene expression (Figs. 5A, C, F), though in some cases suppression of bud development was observed beyond the detectable GFP fluorescence. This may reflect the ability of the receptor extracellular domains to sequester freely diffusing ligand and so act in a non-cell autonomous manner by restricting ligand availability beyond infected regions. The morphological appearance of feather placodes can be visualized by staining with ethidium bromide (Eames and Schneider, 2005). Staining of an embryo infected with DN-cXedar (Figs. 5C, D, E) shows that within the infected tract (Figs. 5D, H), the lateral spread of feather placodes as the tract expands has been arrested, with fewer rows of identifiable placodes compared to the contralateral non-infected tract (Figs. 5E, I). These results agree with the *in vitro* reconstitution studies, indicating that these receptors reinforce placode identity and promote morphogenesis, but they do not appear to be individually required for spatial patterning or initial fate determination.

*In vivo activation of cEdar subfamily signaling*

To determine the effects of ectopic receptor activation, RCAS vectors were used to deliver constitutively active receptor constructs to developing embryos. Introduction of CA-cEdar induced patches of ectopic *cβ-catenin* expression immediately peripheral to the expanding tracts (Figs. 6A, A′). We did not observe ectopic *cβ-catenin* more distant from the tract in the apteric region. This phenotype is very similar to that reported for ectopic *cEdar* expression induced by

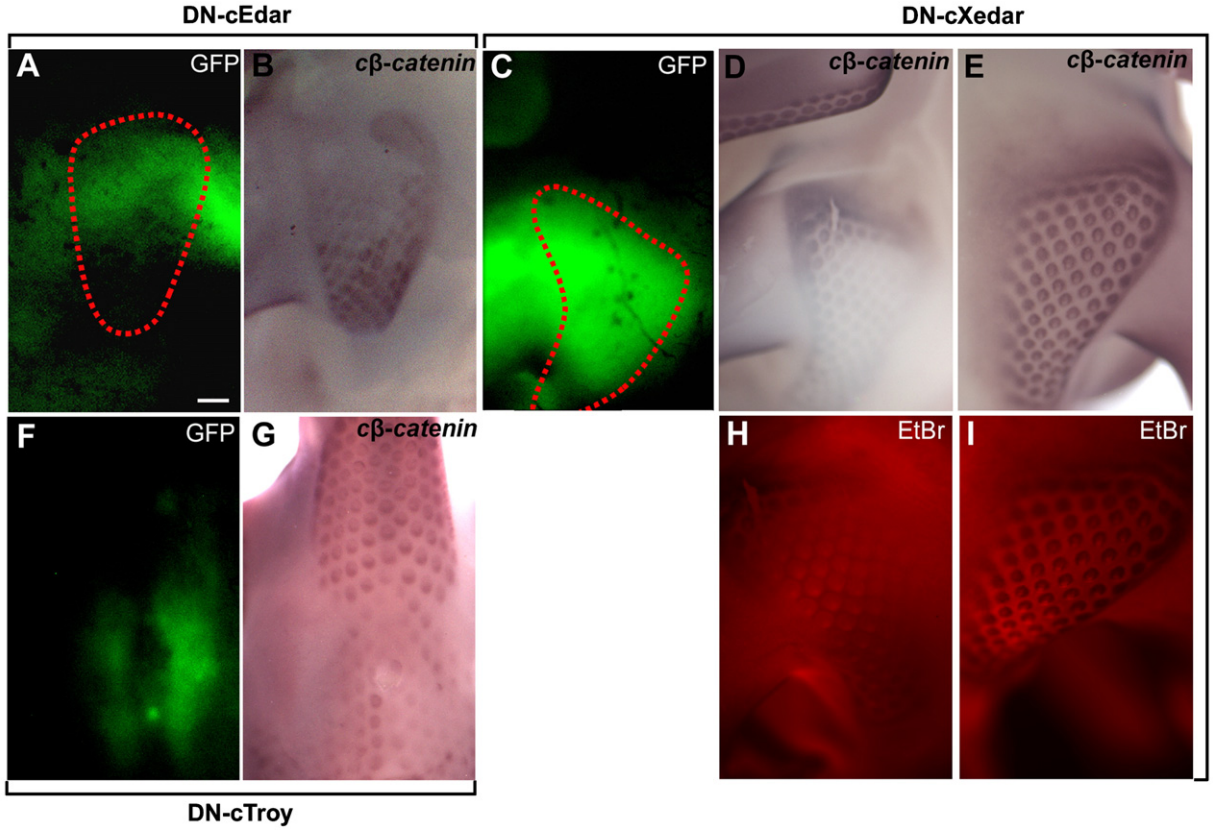


Fig. 5. Suppression of receptor signaling *in vivo*. (A, C, F) GFP fluorescence and (B, D, G) corresponding *cβ-catenin* expression in panels A, B DN-cEdar-, panels C, D DN-cXedar- and panels F, G DN-cTroy-infected embryos. *cβ-Catenin* expression is suppressed in regions expressing dominant negative receptor transgenes. Red dotted lines (A and C) denote presumptive feather tracts. Suppression of placode morphology was demonstrated by staining with ethidium bromide. (D, E, H, I) Embryo infected with DN-cXedar, compare the (D, H) infected tract to the (E, I) contralateral non-infected tract. Scale bar: 200 μm.

activated β-catenin, except that ectopic placodes induced by β-catenin are not limited to the region immediately peripheral to the tract (Houghton et al., 2005). In contrast to CA-cEdar's effects, both CA-cTroy and CA-cXedar generated fusions between buds within the tracts (Figs. 6B, C, C′), but we did not observe ectopic *β-catenin* within or outside the morphogenetic wave. Exclusion of *cEda* expression from these fusions (Fig. 6D) indicates that they have assumed full placode fate and are not cells with a combination of bud and interbud identities. To confirm that the ectopic or fused placode phenotypes observed correlated with foci of infection, embryos post in situ hybridization were cryosectioned, and immunostained for viral gag protein. This demonstrated that within phenotypically abnormal regions viral protein staining was present in both the epithelial and mesenchymal layers of the skin (Figs. 6E, H). In regions of the same embryo where placode phenotype was normal, staining for the viral gag protein was absent (Figs. 6F, I).

### *Suppression of NF-κB in feather bud development*

Edar, Troy and Xedar activate the transcription factor NF-κB (Kojima et al., 2000; Yan et al., 2000), and repression of NF-κB function in the skin of transgenic mice phenocopies *Edar* ablation (Schmidt-Ullrich et al., 2001). To directly test a requirement for NF-κB function in feather development, we treated skin cultures with BAY 11-7082, an inhibitor of IκB phosphorylation (Pierce et al., 1997). Over the 3-day culture period, tract expansion in the control explants resembled the events that occur *in vivo* (Figs. 7A, C, E). In inhibitor-treated

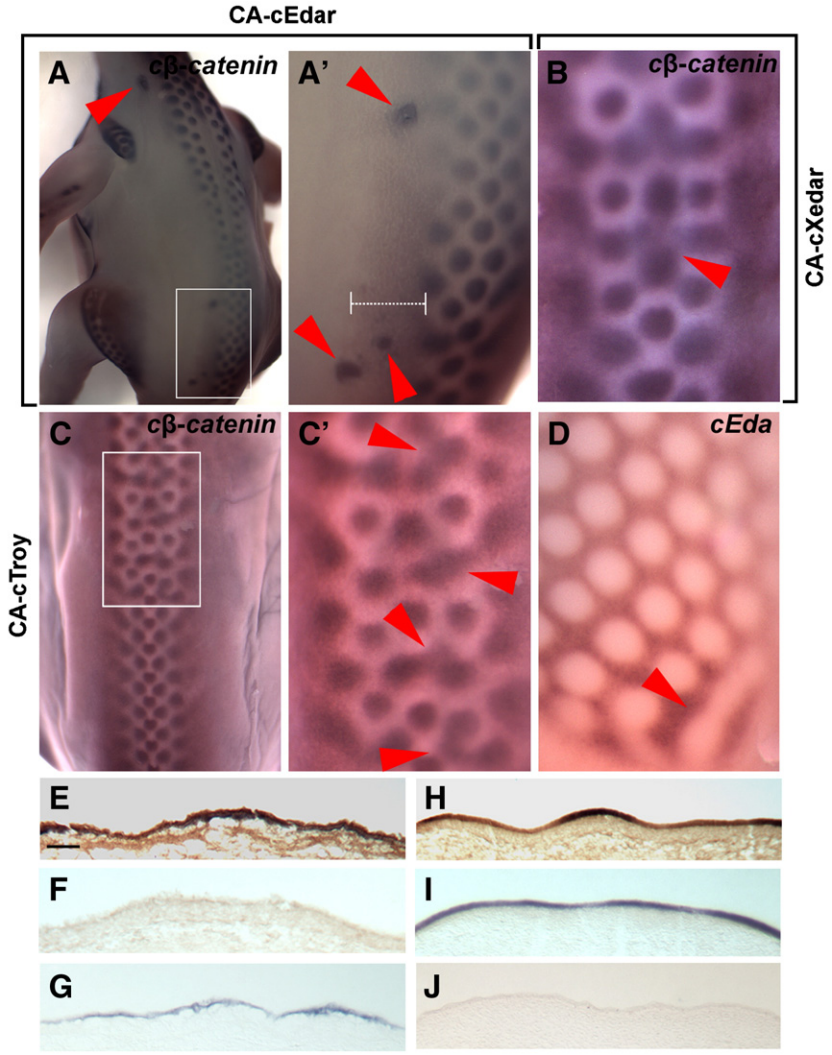


Fig. 6. Activation of receptor signaling *in vivo*. (A) CA-cEdar induces ectopic *cβ-catenin*-expressing foci adjacent to the expanding feather tracts. (A′) Enlargement of the boxed area in panel A. The ectopic foci (arrowheads) are generally circular and stain as intensely as endogenous placodes within the tract. The morphogenetic wave is indicated by a white line. (B) *cβ-Catenin* expression in fused placodes induced by CA-cXedar, arrowhead. (C) CA-cTroy expression causes placode fusions, indicated by *cβ-catenin* expression, within the tracts. (C′) Enlargement of boxed area in panel C. Fusions are indicated by arrowheads. (D) *cEda* expression is excluded from CA-cTroy-induced fusions, arrowhead. (E–I) Retroviral infection detected by anti-gag immunostaining. Embryos had previously been stained to detect *cβ-catenin*. Infection is localised to the epithelium and mesenchyme in panels A, E CA-cEdar- and panels B, H CA-cXedar-infected embryos. (F, I) Regions in these embryos in which phenotype was not apparent do not display positive gag immunostaining. (G) Staining with secondary antibody alone does not exhibit signal in the infected regions. (J) Non-infected control embryo. Scale bar: E–J=250 μm.

explants, the total bud area in the whole explant was reduced. This is manifested as a change in bud density or size, depending on the location within the explant (Figs. 7B, D, F). This finding can be explained by the fact that the feather buds in the midline form before those in lateral rows, thus reflecting stage dependent responses. Placode size towards the midline of the explants was similar to that of the control ($n=12$, Figs. 7D, F, arrowhead). These early feather buds had initiated development at the time when inhibitors were added. Some buds appear to escape the inhibition, while some recede over a 2-day period. More laterally, feather placodes were not established when the inhibitors were added. Here the number of buds was reduced but their size was increased (Figs. 7D, F, arrow, K). This difference is apparent on a scatter plot of bud size relative to location in the skin (midline versus lateral, Fig. 7K). We further examined these buds by in situ hybridization with *cShh*, a known marker of the placode epidermis. In control explants the expression of *cShh* is restricted to the distal epithelium of the long buds (Figs. 7G, I). In the presence of inhibitor, the enlarged buds that had formed also express *cShh*. In these enlarged buds, *cShh* is properly expressed in the distal region of the bud (Figs. 7H, J). Thus although the sizing of the feather buds may be irregular, marker gene expression appears to be normal. In the inhibitor-treated explants, the total bud area of the explant is reduced compared to controls, largely due to a decrease in bud density (Fig. 7K).

## Discussion

We have examined the sequence, expression and functional characteristics of three related receptors of the TNFR superfamily in feather placode development. While the sequence of cEdar is very similar to its human orthologue, cTroy is moderately, and cXedar is highly, divergent from their mammalian counterparts. Our finding of a death domain in cXedar was unexpected, representing to our knowledge the first example of a signaling TNFR which contains a death domain in one lineage but lacks it in another. This finding implies that the ancestral vertebrate Xedar contained a death domain which has been lost in mammals and suggests that Xedar signaling mechanisms are distinct in different vertebrates. The expression patterns of the three receptors are similar to their characteristics in mammalian skin development. In mouse, *Edar* and *Troy* are first expressed throughout the epidermis and then become restricted to the hair placodes (Pispa et al., 2003), and *Xedar* is upregulated slightly later during appendage morphogenesis (Yan et al., 2000). *cEda* is first expressed all over the epidermis, and then becomes restricted to the interbud region in a pattern reciprocal to that of *cEdar*, in an expression pattern resembling that observed in the mouse interfollicular epidermis (Houghton et al., 2005). Thus, with the exception of cXedar, these molecules are expressed in the restrictive mode during skin appendage formation, suggesting a role in the micropatterning process of forming feather buds within tracts (Lin et al., 2006).

While manipulation of receptor and NF-κB signaling activities yielded diverse phenotypes (Fig. 8), some general principles have emerged. We propose that, though not required for the initial assumption of placodal fate, the level of receptor activity modulates both the density and the size of feather buds. Elevated receptor activity leads to a greater fraction of the skin assuming a bud fate, while suppressed signaling has the opposite effect and destabilizes placodes.

The phenotypes caused by expressing dominant negative receptors are not consistent with their being essential for the periodic patterning process. Rather, they appear to regulate epithelial morphogenesis. Our finding that dominant negative cTroy and cXedar suppress feather development is in apparent contrast to their null mutations in mouse, which are reported to cause no gross abnormalities (Shao et al., 2005; Newton et al., 2004). There are several potential explanations for this difference. The first is that the Troy and Xedar mutant mice have subtle defects in hair follicle formation. Given the distinct subtypes of follicles in the mouse coat, it is possible that a significant alteration in the number of any one type would not appear abnormal at a gross level. A second explanation is that Troy and Xedar functions differ between mouse and chicken, an argument perhaps supported by the divergence observed in their protein sequences compared to the high degree of conservation of Edar. The presence of two forms of Troy, a long form capable of signaling and a putative dominant negative short form, suggests a third explanation. While the mouse null mutation ablated both active and antagonistic Troy forms, our dominant negative approach exclusively enhanced the negative Troy function. If Troy functionally interacts with other receptors or signaling pathways, then selective enhancement of negative functions might have more severe consequences than loss of both positive and negative inputs. The essentially identical phenotypes induced by each mutated receptor construct are consistent with such a transdominant negative effect. This effect may be caused by heteromeric Eda ligand complexes recruiting the different receptors into a single signaling complex. Such heteromeric EdaA1–EdaA2 complexes have not been reported, but the presence of a collagen-like domain towards the N-terminus of both Eda variants (Srivastava et al., 1997) suggests that these proteins would be likely to multimerize when coexpressed.

*cXedar* expression is not detectable by in situ hybridization until E10, after the initiation of feather bud morphogenesis. This finding could indicate that the endogenous receptor normally works with cTroy and cEdar to regulate bud shape and growth, but not the early stages of placode formation. That endogenous cXedar might not be as important in placode formation is perhaps supported by the lower efficiency of bud suppression caused by DN-cXedar (26%), compared to the equivalent cEdar (44%) and cTroy (40%) constructs. The phenotypic effects may represent dominant negative inhibition at a time when cXedar signaling may not normally be active, therefore the effects observed may be indicative of ectopic interaction with cEdar and cTroy.

Elevated signaling activity was achieved using LMP1–receptor fusions. Enhanced signaling acting in the morphogenetic zone, where placodes are emerging, led to an increase in bud number. This effect is seen as ectopic bud formation in the morphogenetic wave using CA-cEdar *in vivo*, and increased bud density in the reconstitution assay *in vitro*. If this enhanced activity occurred after placode locations were established it

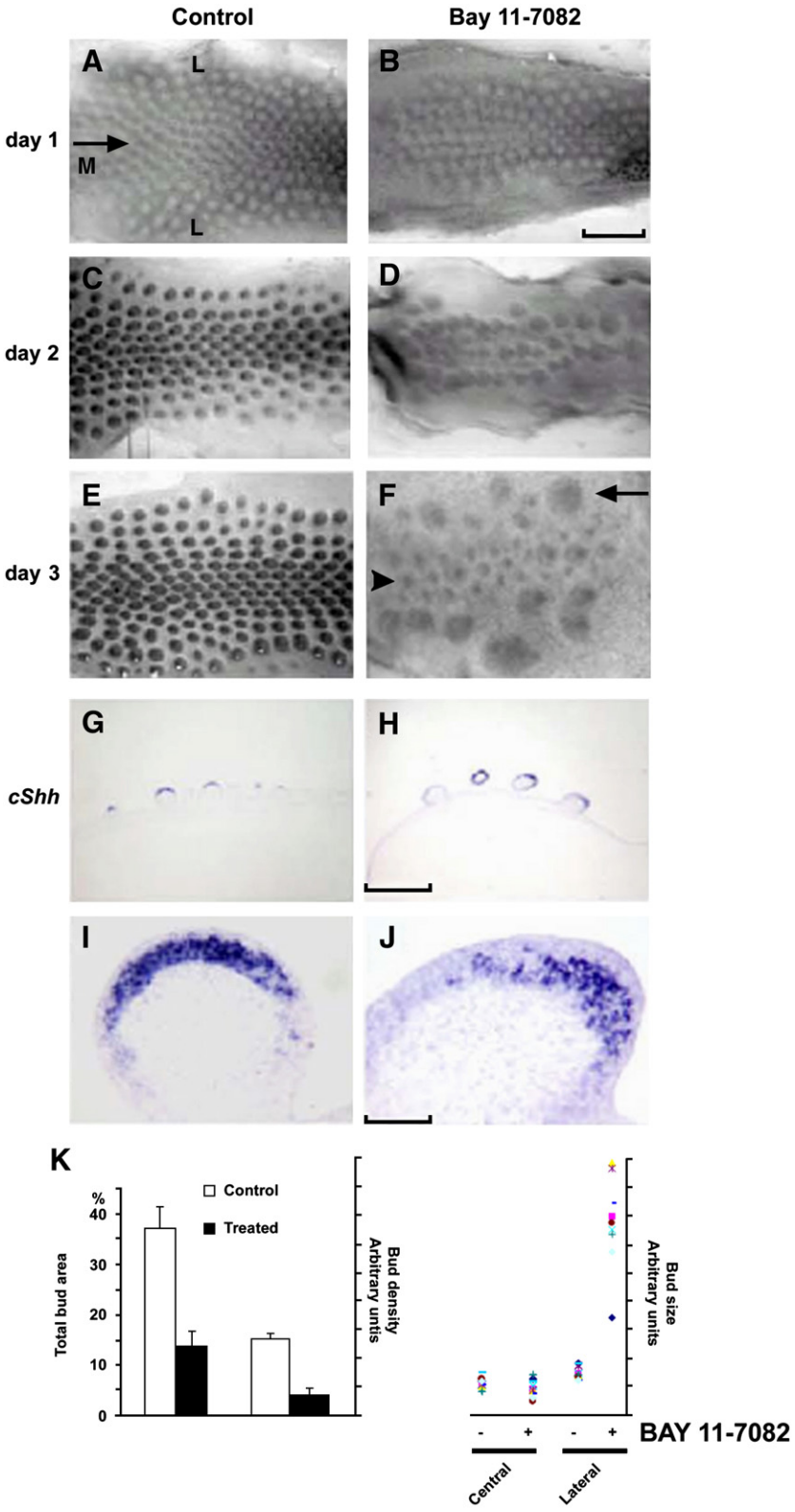


Fig. 7. NF-κB inhibition during feather development. E7 dorsal skin was cultured in the absence or presence of the NF-κB inhibitor, BAY 11-7082. In panels A, C, E control explants long buds begin to form near the midline of the explant (arrow labelled M in panel A), while in panels B, D, F treated explants inhibition of NF-κB results in fewer buds and large interbud spacing. Placodes near the midline are more advanced than lateral ones (L in panel A) when drug is added. (F) Lateral placodes enlarge in size but reduce in number (arrow) compared to medial placodes (arrowhead). (G, I) Expression of *cShh* shows localisation to the distal edges at the tips of the control long buds. (H, J) *cShh* is appropriately expressed in the buds which form in the BAY 11-7082-treated explants. (K) Quantification of the fraction of skin occupied by feather buds and overall bud density in explants. Error bars indicate standard deviation. The right panel shows a scatter plot comparing buds from the midline (equivalent to the control explant, central row and 3 rows on each side) and lateral regions, respectively. Scale bars: A–F = 1000 μm; G, H = 500 μm; I, J = 50 μm.

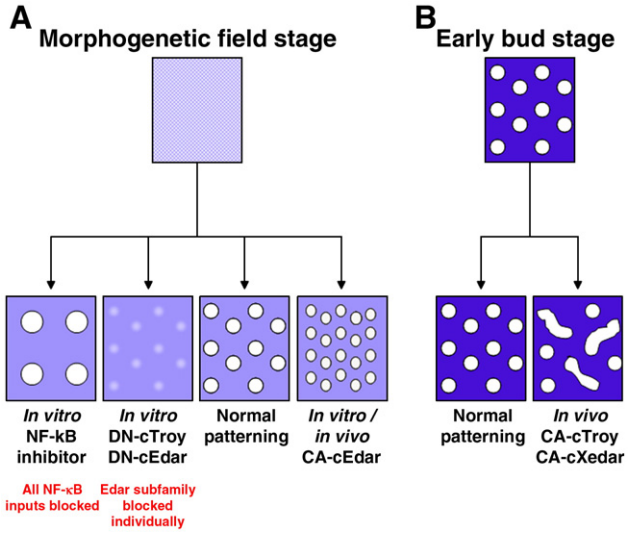


Fig. 8. Model for roles of receptor and NF-κB signaling at different stages of feather development. (A) Modulation of receptor/NF-κB activity during periodic patterning leads to the alteration of placode density. This is represented in the lateral edges of BAY 11-7082-treated explants which display a low density of enlarged buds. When receptor activities are modulated individually in reconstitution assays, epithelial placode formation and bud outgrowth is suppressed. Hyperactivated cEdar induces a higher bud density in reconstitution assays and ectopic buds *in vivo*. (B) Modulation of signaling after placodes form. Feather bud size is affected, with larger fused buds caused by hyperactivation of cTroy or cXedar signaling.

instead converted some interbud domains to bud by increasing bud size, leading to placode fusions as seen using CA-cTroy and CA-cXedar.

*In vivo*, cEdar generated ectopic buds in the morphogenetic wave, ahead of agreed placode locations, while cTroy and cXedar promoted placode fusion within tracts. The reason for this difference is unclear, but may reflect when and where these receptors act relative to the inhibitors of placode fate. If cEdar acts upstream of the inhibitors, and its signaling is susceptible to their action, then this would explain the lack of intratract fusions observed. That Edar itself is susceptible to the inhibitory effects of BMP signaling has been shown in mouse and chick (Houghton et al., 2005; Mou et al., 2006), though whether its cytoplasmic signal transduction apparatus is also inhibited by these factors remains to be tested. Conversely, cTroy and cXedar may act downstream of the inhibitors, evading lateral inhibitory signals emanating from the placodes and allowing fusions to form within the tracts. It is also possible that signaling pathways other than NF-κB are differentially activated by these three receptors, and that this divergence in downstream signal transduction is the cause of the spatially distinct phenotypes caused by the activated receptors. The weak NF-κB activation induced by CA-cXedar *in vitro* might support the notion that other signaling pathways are employed by these receptors.

Overexpression of EdaA2 in mouse has been reported to have no effect on skin or appendage development (Newton et al., 2004), suggesting that restricted receptor expression, rather than ligand availability, is the primary mode of regulating of this pathway. Stimulation of Edar signaling by application of recombinant EdaA1 to embryonic mouse skin cultures has been reported to cause enlarged, fused hair placodes (Mustonen et al., 2004). This phenotype is similar to that we find caused by activation of cTroy and cXedar, but not by cEdar. Though similar in ultimate appearance, the mechanisms of hair and feather placode fusion may be distinct. Hair placode fusion is a result of the joining of independently generated placodes, each of which is approximately the same age. Since feathers are generated as the morphogenetic wave sweeps laterally across the skin, fusions in this system are between older and younger buds, and are most likely caused by a failure of separation rather than the union of two initially distinct placodes.

Suppression of pathway activity was achieved by expressing dominant negative receptors or by pharmacological inhibition of NF-κB activity. When suppression by dominant negative receptors took place at the morphogenetic wave stage, in the reconstitution system, there was an overall suppression of bud formation, although the stable dermal condensation of the feather primordium was visible. The dermal papilla condensates appeared periodically patterned, though a morphologically distinct epithelial placode did not appear and bud outgrowth did not occur. This finding in chicken skin is in apparent contrast to the situation in the Edar pathway mouse mutants, where some effort at epithelial placode formation seems to occur without formation of a distinct dermal papilla (Schmidt-Ullrich et al., 2006). This may indicate a difference in the relative contributions of dermal and epidermal components to early appendage formation in the different species, with the dermis being more clearly predominant in feather development.

NF-κB has been identified as a promoter of placodal fate in mouse (Schmidt-Ullrich et al., 2006). Pharmacological inhibition of NF-κB in explant cultures allows an analysis of its roles in the formation of the feather primordia. We were able to determine the phenotypic effects of blockade of all signals activating this transcription factor as an addition to dominant negative inhibition of individual receptor signaling. When NF-κB inhibition occurs at a stage when feather primordia are already formed (the central rows of the feather explant), suppression of NF-κB leads to some of the midline buds receding over a 2-day period. When NF-κB inhibition acts at a stage when periodic patterning is still ongoing (in the lateral regions of the explant), there is an overall reduction in the number of feather placodes. These “reset buds” are larger than normal buds possibly due to the increase in interbud spacing and lack of inhibitory signals from the surrounding placodes.

Phenotypic effects resulting from the blockade of NF-κB activity are more pronounced than those generated by expression of individual dominant negative receptors. That inhibition of all NF-κB activating inputs has this stronger effect suggests that there are other factors that activate NF-κB during feather morphogenesis, or else that the three receptors analysed here have redundant functions relative to one another. Taken together, these data from both *in vivo* and *in vitro* models suggest that the Edar subfamily–NF-κB axis plays an important role in setting the number of buds formed during the initial pattern forming stage, and regulates bud size during early feather bud morphogenesis.

Of the genes known to regulate appendage development, β-catenin is the most intensively studied and has produced the most dramatic phenotypes when manipulated in developing skin. Expression of activated β-catenin in embryonic chicken skin causes ectopic placodogenesis and feather growth (Noramly et al., 1999; Houghton et al., 2005). The ectopic placodes express *cEdar* (Houghton et al., 2005), a point that has been used to suggest that β-catenin lies upstream of Edar in a linear developmental pathway. Our finding that cEdar can upregulate β-catenin expression indicates that this linear model for placode initiation may not be tenable, or at least that evidence obtained from gain of function experiments is insufficient to draw these conclusions. Rather, genes expressed in the restrictive mode prior to placode formation appear to be mutually reinforcing, a phenomenon that would help achieve threshold levels of activation required to assume a placode fate. β-Catenin has a greater range of placode-inducing ability, being able to produce buds in essentially any location in the skin, while we observed cEdar-induced buds only in the morphogenetic wave bordering the developing tracts. This spatial characteristic may simply reflect the distribution of signaling co-factors, with full cEdar signal transduction requiring co-expression of cEdaradd, which is restricted to the buds and the morphogenetic wave (Houghton et al., 2005).

Data from mammals, fish and birds indicates that Edar's sequence and function are conserved across the vertebrate classes (Kondo et al., 2001; Houghton et al., 2005). Thus a highly constrained Edar perhaps lies at the core of an ancestral skin appendage development programme. Troy and Xedar are more extensively diverged, indicating that they may be more peripheral to this programme and thus more malleable evolutionary agents. Importantly the retention of the death domain in Xedar in the avian genome will be addressed by examination of the function of the domain both biochemically and *in vivo*. Future study of the Edar subfamily will dissect their interactions, aiming to illustrate the uses to which duplicated genes may be put in order to generate the complex organ forms we see today.

## Acknowledgments

We thank Keith Brennan, Heithem El-Hodiri, David Garrod, Stacie Loftus, Karen More, Pascal Schneider, Bill Sugden, Cheryll Tickle and Randall B. Widelitz. This work was supported by funding from the BBSRC, UK (DJH) and NIAMS AR 042177 and 047364 from NIH, USA (CMC).

## References

Boardman, P.E., Sanz-Ezquerro, J., Overton, I.M., Burt, D.W., Bosch, E., Fong, W.T., Tickle, C., Brown, W.R., Wilson, S.A., Hubbard, S.J., 2002. A comprehensive collection of chicken cDNAs. Curr. Biol. 12, 1965–1969.

Bossen, C., Ingold, K., Tardivel, A., Bodmer, J.L., Gaide, O., Hertig, S., Ambrose, C., Tschopp, J., Schneider, P., 2006. Interactions of tumor necrosis factor TNF and TNF receptor family members in the mouse and human. J. Biol. Chem. 281, 13964–13971.

Botchkarev, V.A., Botchkareva, N.V., Sharov, A.A., Funa, K., Huber, O., Gilchrest, B.A., 2002. Modulation of BMP signaling by noggin is required for induction of the secondary (nontylotrich) hair follicles. J. Invest. Dermatol. 118, 3–10.

Chang, C.H., Jiang, T.X., Lin, C.M., Burrus, L.W., Chuong, C.M., Widelitz, R., 2004. Distinct Wnt members regulate the hierarchical morphogenesis of skin regions spinal tract and individual feathers. Mech. Dev. 121, 157–171.

Eames, B.F., Schneider, R.A., 2005. Quail-duck chimeras reveal spatiotemporal plasticity in molecular and histogenic programs of cranial feather development. Development 132, 1499–1509.

Fuchs, E., Merrill, B.J., Jamora, C., DasGupta, R., 2001. At the roots of a never-ending cycle. Dev. Cell 1, 13–25.

Hardy, M.H., 1992. The secret life of the hair follicle. Trends Genet. 8, 55–61.

Hatzivassiliou, E., Miller, W.E., Raab-Traub, N., Kieff, E., Mosialos, G., 1998. A fusion of the EBV latent membrane protein-1 LMP1 transmembrane domains to the CD40 cytoplasmic domain is similar to LMP1 in constitutive activation of epidermal growth factor receptor expression, nuclear factor-kappa B, and stress-activated protein kinase. J. Immunol. 160, 1116–1121.

Headon, D.J., Overbeek, P.A., 1999. Involvement of a novel TNF receptor homologue in hair follicle induction. Nat. Genet. 22, 370–374.

Headon, D.J., Emmal, S.A., Ferguson, B.M., Tucker, A.S., Justice, M.J., Sharpe, P.T., Zonana, J., Overbeek, P.A., 2001. Gene defect in ectodermal dysplasia implicates a death domain adapter in development. Nature 414, 913–916.

Houghton, L., Lindon, C., Morgan, B.A., 2005. The ectodysplasin pathway in feather tract development. Development 132, 863–872.

Inoue, J., Ishida, T., Tsukamoto, N., Kobayashi, N., Naito, A., Azuma, S., Yamamoto, T., 2000. Tumor necrosis factor receptor-associated factor (TRAF) family: adapter proteins that mediate cytokine signaling. Exp. Cell Res. 254, 14–24.

Jiang, T.X., Jung, H.S., Widelitz, R.B., Chuong, C.M., 1999. Self-organization of periodic patterns by dissociated feather mesenchymal cells and the regulation of size, number and spacing of primordia. Development 126, 4997–5009.

Jiang, T.X., Widelitz, R.B., Shen, W.M., Will, P., Wu, D.Y., Lin, C.M., Jung, H.S., Chuong, C.M., 2004. Integument pattern formation involves genetic and epigenetic controls: feather arrays simulated by digital hormone models. Int. J. Dev. Biol. 48, 117–135.

Kanda, H., Igaki, T., Kanuka, H., Yagi, T., Miura, M., 2002. Wengen, a member of the *Drosophila* tumor necrosis factor receptor superfamily, is required for Eiger signaling. J. Biol. Chem. 277, 28372–28375.

Kere, J., Srivastava, A.K., Montonen, O., Zonana, J., Thomas, N., Ferguson, B., Munoz, F., Morgan, D., Clarke, A., Baybayan, P., Chen, E.Y., Ezer, S., Saarialho-Kere, U., de la Chapelle, A., Schlessinger, D., 1996. X-linked anhidrotic hypohidrotic ectodermal dysplasia is caused by mutation in a novel transmembrane protein. Nat. Genet. 13, 409–416.

Kojima, T., Morikawa, Y., Copeland, N.G., Gilbert, D.J., Jenkins, N.A., Senba, E., Kitamura, T., 2000. TROY, a newly identified member of the tumor necrosis factor receptor superfamily, exhibits a homology with Edar and is expressed in embryonic skin and hair follicles. J. Biol. Chem. 275, 20742–20747.

Kondo, S., Kuwahara, Y., Kondo, M., Naruse, K., Mitani, H., Wakamatsu, Y., Ozato, K., Asakawa, S., Shimizu, N., Shima, A., 2001. The medaka rs-3 locus required for scale development encodes ectodysplasin–A receptor. Curr. Biol. 11, 1202–1206.

Laurikkala, J., Pispa, J., Jung, H.S., Nieminen, P., Mikkola, M., Wang, X., Saarialho-Kere, U., Galceran, J., Grosschedl, R., Thesleff, I., 2002. Regulation of hair follicle development by the TNF signal ectodysplasin and its receptor Edar. Development 129, 2541–2553.

Lin, C.M., Jiang, T.X., Widelitz, R.B., Chuong, C.M., 2006. Molecular signaling in feather morphogenesis. Curr. Opin. Cell Biol. 18, 730–741.

Locksley, R.M., Killeen, N., Lenardo, M.J., 2001. The TNF and TNF receptor superfamilies: integrating mammalian biology. Cell 104, 487–501.

Loftus, S.K., Larson, D.M., Watkins-Chow, D., Church, D.M., Pavan, W.J., 2001. Generation of RCAS vectors useful for functional genomic analyses. DNA Res. 8, 221–226.

Millar, S.E., 2002. Molecular mechanisms regulating hair follicle development. J. Invest. Dermatol. 118, 216–225.

Mou, C., Jackson, B., Schneider, P., Overbeek, P.A., Headon, D.J., 2006. Generation of the primary hair follicle pattern. Proc. Natl. Acad. Sci. U. S. A. 103, 9075–9080.

Mustonen, T., Ilmonen, M., Pummila, M., Kangas, A.T., Laurikkala, J., Jaatinen, R., Pispa, J., Gaide, O., Schneider, P., Thesleff, I., Mikkola, M.L., 2004.

Ectodysplasin A1 promotes placodal cell fate during early morphogenesis of ectodermal appendages. Development 131, 4907–4919.

Newton, K., French, D.M., Yan, M., Frantz, G.D., Dixit, V.M., 2004. Myodegeneration in EDA-A2 transgenic mice is prevented by XEDAR deficiency. Mol. Cell. Biol. 24, 1608–1613.

Noramly, S., Freeman, A., Morgan, B.A., 1999. beta-Catenin signaling can initiate feather bud development. Development 126, 3509–3521.

Pierce, J.W., Schoenleber, R., Jesmok, G., Best, J., Moore, S.A., Collins, T., Gerritsen, M.E., 1997. Novel inhibitors of cytokine-induced IkappaBalpha phosphorylation and endothelial cell adhesion molecule expression show anti-inflammatory effects in vivo. J. Biol. Chem. 272, 21096–21103.

Pispa, J., Mikkola, M.L., Mustonen, T., Thesleff, I., 2003. Ectodysplasin, Edar and TNFRSF19 are expressed in complementary and overlapping patterns during mouse embryogenesis. Gene Expr. Patterns. 3, 675–679.

Plikus, M., Wang, W.P., Liu, J., Wang, X., Jiang, T.X., Chuong, C.M., 2004. Morpho-regulation of ectodermal organs: integument pathology and phenotypic variations in K14-Noggin engineered mice through modulation of bone morphogenic protein pathway. Am. J. Pathol. 164, 1099–1114.

Riddle, R.D., Johnson, R.L., Laufer, E., Tabin, C., 1993. Sonic hedgehog mediates the polarizing activity of the ZPA. Cell 75, 1401–1416.

Schmidt-Ullrich, R., Aebischer, T., Hulsken, J., Birchmeier, W., Klemm, U., Scheidereit, C., 2001. Requirement of NF-kappaB/Rel for the development of hair follicles and other epidermal appendices. Development 128, 3843–3853.

Schmidt-Ullrich, R., Tobin, D.J., Lenhard, D., Schneider, P., Paus, R., Scheidereit, C., 2006. NF-kappaB transmits Eda A1/EdaR signalling to activate Shh and cyclin D1 expression, and controls post-initiation hair placode down growth. Development 133, 1045–1057.

Schneider, P., Street, S.L., Gaide, O., Hertig, S., Tardivel, A., Tschopp, J., Runkel, L., Alevizopoulos, K., Ferguson, B.M., Zonana, J., 2001. Mutations leading to X-linked hypohidrotic ectodermal dysplasia affect three major functional domains in the tumor necrosis factor family member ectodysplasin-A. J. Biol. Chem. 276, 18819–18827.

Sengel, P., 1990. Pattern formation in skin development. Int. J. Dev. Biol. 34, 33–50.

Shao, Z., Browning, J.L., Lee, X., Scott, M.L., Shulga-Morskaya, S., Allaire, N., Thill, G., Levesque, M., Sah, D., McCoy, J.M., Murray, B., Jung, V., Pepinsky, R.B., Mi, S., 2005. TAJ/TROY, an orphan TNF receptor family member, binds Nogo-66 receptor 1 and regulates axonal regeneration. Neuron 45, 353–359.

Srivastava, A.K., Pispa, J., Hartung, A.J., Du, Y., Ezer, S., Jenks, T., Shimada, T., Pekkanen, M., Mikkola, M.L., Ko, M.S., Thesleff, I., Kere, J., Schlessinger, D., 1997. The Tabby phenotype is caused by mutation in a mouse homologue of the *EDA* gene that reveals novel mouse and human exons and encodes a protein (ectodysplasin-A) with collagenous domains. Proc. Natl. Acad. Sci. U. S. A. 94, 13069–13074.

Thesleff, I., Mikkola, M.L., 2002. Death receptor signaling giving life to ectodermal organs. Sci. STKE E22.

van Genderen, C., Okamura, R.M., Farinas, I., Quo, R.G., Parslow, T.G., Bruhn, L., Grosschedl, R., 1994. Development of several organs that require inductive epithelial–mesenchymal interactions is impaired in LEF-1-deficient mice. Genes Dev. 8, 2691–2703.

Wajant, H., 2003. Death receptors. Essays Biochem. 39, 53–71.

Widelitz, R.B., Jiang, T.X., Lu, J., Chuong, C.M., 2000. Beta-catenin in epithelial morphogenesis: conversion of part of avian foot scales into feather buds with a mutated beta-catenin. Dev. Biol. 219, 98–114.

Wu, P., Hou, L., Plikus, M., Hughes, M., Scehnet, J., Suksaweang, S., Widelitz, R., Jiang, T.X., Chuong, C.M., 2004. Evo–Devo of amniote integuments and appendages. Int. J. Dev. Biol. 48, 249–270.

Yan, M., Wang, L.C., Hymowitz, S.G., Schilbach, S., Lee, J., Goddard, A., de Vos, A.M., Gao, W.Q., Dixit, V.M., 2000. Two-amino acid molecular switch in an epithelial morphogen that regulates binding to two distinct receptors. Science 290, 523–527.

Yan, M., Zhang, Z., Brady, J.R., Schilbach, S., Fairbrother, W.J., Dixit, V.M., 2002. Identification of a novel death domain-containing adaptor molecule for ectodysplasin-A receptor that is mutated in crinkled mice. Curr. Biol. 12, 409–413.

Yu, M., Yue, Z., Wu, P., Wu, D.Y., Mayer, J.A., Medina, M., Widelitz, R.B., Jiang, T.X., Chuong, C.M., 2004. The biology of feather follicles. Int. J. Dev. Biol. 48, 181–191.